Asian Journal of Chemistry Vol. 18, No. 3 (2006), 2269–2279

The H + D_2 → HD + D and D + H_2 → HD + H Reactions: *ab initio* and Rate Constants Calculations

M. DEHESTANI* and F. SHOJAIE
Department of Chemistry, Shahid Bahonar University
P.O. Box 76169-133, Kerman, Iran
E-mail: dehestani2002@yahoo.com

The ab initio calculations have been carried out on the H + D_2 → HD + D and D + H_2 → HD + H reactions. Geometry optimization, vibrational frequency and energy calculations have been performed on all reactants and the transition states using the Gaussian 98 set of quantum chemistry codes at different levels of *ab initio* theory. The *ab initio* frequencies and geometries for H_2 and D_2, calculated at the QCISD/cc-PVTZ and QCISD/aug-cc-PVTZ levels of theory, are in very good agreement with experiment. The *ab initio* normal mode frequencies and geometries for the transition states are similar to those for the double many-body expansion surface. Based on these *ab initio* calculations, conventional transition state theory, thermodynamic formulation of transition state theory and semiclassical transition state theory have been used to predict the rate constants as function of temperature (300–1100 K). With QCISD/cc-PVTZ and QCISD/aug-cc-PVTZ levels, the calculated rate constants are in reasonable agreement with their experimental counterparts.

Key Words: *ab initio* calculations, Transition state theory, Semi-classical state theory.

INTRODUCTION

The isotope-exchange reactions of atomic and molecular hydrogen are small real molecular systems in three-dimensional space and have always been of fundamental importance for comparison of experiment and theory in chemical kinetics.

Experimental rate constants and their ratio have been measured for the istopic hydrogen-atom-molecule reaction, over a wide range of temperatures[1–3]. Jayaweera and Pacey[4] determined the rate constant H + D_2 (v = 0) reaction at the temperature range down to 256 K by using an electron spin resonance technique. The rate constants for this reaction[5] and D + H_2 (v = 0) were measured, over the temperature range 655–1979 K, by Michael *et al.*[6]. Different techniques were applied to measure the rate constants of H + H_2 (v = 1) and D + H_2 (v = 1) reactions[7, 8]. The quasi-classical trajectories (QCT) calculation of the rate constant on the potential energy surface of Porter and Karplus[9] was performed for the deuterated isotopic variants of the reaction[10]. Dynamical calculations of QCT

were applied for the H + H_2, D + H_2, H + D_2 reactions on the the Liu-Siegbahn-Truhlar-Horowitz potential energy surface (LSTH)[11] by Mayne and co-workers[12]. Quickert and Le Roy[3] computed the rate constant ratio for the hydrogen-exchange reactions by transition state theory with quantum mechanical tunneling. Rate constants were computed for these reactions using the conventional transition state theory and canonical variational theory by Garret and co-workers[13]. The constant centrifugal potential method was carried out for calculation of rate constants of D + H_2 (v = 0, j = 0) by Takada *et al.*[14]. Approximate theoretical[15, 16] and accurate quantum mechanical[17, 18] calculations for the D + H_2 (v = 0, 1) reaction on the surfaces of LSTH, double many-body expansion (DMBE) of Varandas *et al.*[19] and of Boothroyd *et al.*[20] surfaces have been performed by several groups over the temperature range 167–1500 K. Accurate quantum mechanical calculations were carried out for the determination of thermal rate constants of the D + H_2 (v = 1, j = 0–3) reaction up to 500 K by Auerbach and Miller[21]. Aoiz *et al.*[22] used a QCT method on the three *ab initio* potential energy surfaces LSTH, DMBE and BKMP to calculate the thermal rate constants for the D + H_2 (v = 0–1, j = 0–7) reaction. Yamamoto and Miller[23] applied the semi-classical initial-value representation (SC-IVR) method to calculate the thermal rate constant for the D +H_2 reaction.

In the present work, we present geometry optimization, harmonic vibrational frequency, barrier height calculation for the H + D_2 and D + H_2 reactions, by using up to date density functional calculation with a large set of basis set functions. We also present the thermal rate constants of these reactions using a potential energy surface fitted to our best *ab initio* calculations with three methods, the conventional transition state theory (CTST), thermodynamic formulation of transition state theory (TFTST) and semi-classical transition state theory (SCTST) introduced by Miller *et al.*[24]

Computational procedures

We have used three methods, conventional transition state theory (CTST), thermodynamic formulation of transition state theory (TFTST) and semiclassical transition state theory (SCTST) that had been employed to calculate rate constant of reaction of H + H_2 in our previous paper[25].

The geometry and the harmonic vibrational frequencies of H_2, D_2, DH_2 and HD_2 at the hybrid density functional B3LYP, Moller-Plesset correlation energy correction MP2, quadratic configuration interaction method (QCISD), coupled cluster doubles method (CCD), couper cluster singles and doubles method (CCSD) and configuration interaction double method (CID) were calculated using the 6-31+G*, 6-311G**, cc-PVDZ, cc-PVTZ, aug-cc-PVDZ and aug-cc-PVTZ basis sets. These calculations were performed employing the Guassian 98 suite of programs[26].

RESULTS AND DISCUSSION

The geometries and *ab initio* harmonic frequencies for H_2 and D_2 calculated at the level QCISD with cc-PVTZ and aug-cc-PVTZ basis sets, are in very good agreement with the experimental structure ($R_{HH} = R_{DD} = 0.741$ Å) and harmonic vibrational frequency ($\omega_{H_2} = 4401$ cm^{-1} and $\omega_{D_2} = 3112$ cm^{-1})[19]. As seen in Tables

1 and 2, in the transition state of H + D_2 reaction, at the level QCISD with basis sets cc-PVTZ and aug-cc-PVTZ, bond lengths, vibrational frequencies and classical barrier heights are in very good agreement with results DMBE surface[19]. Present *ab initio* calculations at this level with basis sets cc-PVTZ and aug-cc-PVTZ of the HD_2 potential energy surface give a linear transition state with the same band distances $R_{HD} = R_{DD} = 0.9301$ and 0.9313 Å, classical reaction barriers (*i.e.*, energy of the transition state with respect to the minimum of the isolated D_2 potential) of 10.27 and 10.05 kcal/mol, respectively. The DMBE surface found the bond lengths and classical reaction barriers at transition state to be 0.929 Å and 9.8 kcal/mol, respectively. Since the level QCISD with basis sets cc-PVTZ and aug-cc-PVTZ can provide perfect results in geometries, vibrational frequencies and barrier height, they are employed to calculate rate constants of the H + D_2 and D + H_2 reactions.

TABLE-1
AB INITIO MINIMUM-ENERGY GEOMETRIES AND VIBRATIONAL FREQUENCIES FOR THE H + D_2 REACTION

Properties			QCISD		
			cc-PVTZ[c]	aug-cc-PVTZ[d]	Reference [31]
Bond length[a]	D_2		0.7426	0.7430	0.741
	TS		0.9301	0.9313	0.929
Frequencies[b]	D_2	ω	3130.0830	3124.2337	3112
	TS	ω_1	1767.6099	1763.4259	1777.6
		ω_2	702.4132	676.4953	686.6
		ϖ_4	1153.9369	1154.8278	1120.6

[a]Distances are in Å. Bond angle (D, X, D) is 90° and dihedral angle (D, X, D, H) is 180° for transition state (TS).
[b]The harmonic frequencies are in units of cm^{-1}. ω_1 = frequencies of symmetric stretch, ω_2 = frequencies of degenerate bend, ϖ_4 = frequencies of the imaginary reaction mode of transition state (HD_2).
[c]This work is in basis set cc-PVTZ.
[d]This work is in basis set aug-cc-PVTZ.

TABLE-2
AB INITIO ENERGIES FOR THE H + D_2 REACTION

Properties		QCISD	
		cc-PVTZ[c]	aug-cc-PVTZ[d]
Electronic energies	H + D_2	1.672146	1.672457
	TS	1.655777	1.656443
Reaction energies	E_0^a	10.27171	10.04875
	E_0^b	10.33193	10.03746

The electronic energies are in units hartrees (negative).
[a]The classical reaction energies ($kcal/mol^{-1}$) do not include zero-point energies.
[b]The quantum reaction energies ($kcal/mol^{-1}$) including zero-point energies.
[c]This work is in basis set cc-PVTZ.
[d]This work is in basis set aug-cc-PVTZ.

The present *ab initio* calculations, as well as three methods discussed in section of theory, were employed to calculate rate constant of the $H + D_2$ reaction. First, the calculations using CTST method with Eckart tunneling and with statistical factor have been performed. From *ab initio* calculation results, complete transitionrotation-vibration-electronic partition functions of the activated complex (HD_2), reactants (H and D_2) and tunneling correction were calculated, then the rate constants were calculated with tunneling effect and with statistical effect ($L^{\pm} = 2$) at each temperature. The comparison between these results with the results of other works and experimental values is represented in Table-3. As seen, the CTST k(T) with tunneling correction from *ab initio* calculations at QCISD level and basis set aug-cc-PVTZ agree with results of Park and Light[27], Garret and Truhlar[28], Michae and Fisher[29] and the experimental data[30] at low temperatures. However, since the tunneling effect is not important at high temperatures, CTST including this correction cannot reproduce the good results for temperatures larger than 400 K. The agreement between quantum rate constants and the CTST results with statistical factor is better than the ones with tunneling effect at the high temperatures. Then to obtain thermal rate constants for this reaction using TFTST with Eckart tunneling and with statistical factor, it was necessary to have thermodynamic functions of transition state. The *ab initio* calculations were used to determine the standard enthalpy and entropy changes at each temperature. Of these properties, the rate constants were calculated at different temperatures and compared with quantum results[30] in Table-4.

TABLE-3
COMPARISON OF CTST RATE CONSTANTS (cm^3 $molecule^{-1}$ s^{-1}) FOR THE $H + D_2$ REACTION OF THIS WORK WITH OTHER RESULTS AND THE EXPERIMENT

T (K)	k(T) [Ref. 27]	k(T) [Ref. 28]	k(T) [Ref. 29]	k(T) exp [Ref. 30]	k(T) QCISD[b]	k(T) QCISD[c]	k(T) QCISD[d]	k(T) QCISD[e]
300	1.7 (–17)[a]	1.55 (–17)	1.82 (–17)	2.1 (–17)	1.44 (–17)	1.22 (–17)	1.63 (–17)	1.38 (–17)
400	—	5.61 (–16)	7.23 (–16)	7.2 (–16)	5.01 (–16)	5.65 (–16)	5.45 (–16)	6.15 (–16)
500	5.6 (–15)	—	6.59 (–15)	6.8 (–15)	3.91 (–15)	5.19 (–15)	4.15 (–15)	5.51 (–15)
600	—	3.61 (–14)	2.88 (–14)	3.2 (–14)	1.46 (–14)	2.15 (–14)	1.52 (–14)	2.24 (–14)
700	7.8 (–14)	—	8.24 (–13)	1.0 (–13)	3.58 (–14)	5.66 (–14)	3.69 (–14)	5.82 (–14)
800	—	—	1.81 (–13)	2.6 (–13)	6.84 (–14)	1.13 (–13)	6.96 (–14)	1.15 (–13)
900	3.7 (–13)	—	3.35 (–13)	5.4 (–13)	1.10 (–13)	1.89 (–13)	1.12 (–13)	1.91 (–13)
1000	—	7.9 (–13)	5.48 (–13)	9.9 (–13)	1.58 (–13)	2.78 (–13)	1.59 (–13)	2.79 (–13)

[a] $1.7(-17) = 1.7 \times 10^{-17}$.
[b, c] This work is in basis set cc-PVTZ with tunneling correction and statistical factor, respectively.
[d, e] This work is in basis set aug-cc-PVTZ with tunneling correction and statistical factor, respectively.

TABLE-4
COMPARISON OF TFTST THERMAL RATE CONSTANT (cm^3 $molecule^{-1}$ s^{-1}) FOR THE H + D_2 REACTION OF THIS WORK WITH QUANTUM RESULTS

T (K)	k(T) [Ref. 30][a]	k(T) QCISD[b]	k(T) QCISD[c]	k(T) QCISD[d]	k(T) QCISD[e]
300	4.9 (–19)	1.167 (–19)	7.943 (–20)	1.399 (–19)	1.037 (–19)
400	—	3.323 (–18)	3.724 (–18)	4.360 (–18)	4.909 (–18)
500	9.0 (–17)	3.624 (–17)	5.943 (–17)	3.588 (–17)	7.780 (–17)
600	—	1.989 (–16)	2.933 (–16)	2.032 (–16)	3.639 (–16)
700	8.1 (–16)	6.615 (–16)	9.221 (–16)	6.934 (–16)	1.027 (–15)
800	—	1.473 (–15)	2.199 (–15)	1.502 (–15)	2.278 (–15)
900	2.6 (–15)	2.776 (–15)	4.359 (–15)	2.860 (–15)	4.459 (–15)
1000	—	4.554 (–15)	7.589 (–15)	4.677 (–15)	7.621 (–15)

[a]Quantum result.
[b, c]This work is in basis set cc-PVTZ with tunneling correction and statistical factor, respectively.
[d, e]This work is in basis set aug-cc-PVTZ with tunneling correction and statistical factor, respectively.

Finally, thermal rate constants for zero total angular momentum were calculated between 300 and 1100 K using SCTST. Table-5 compares the rate constants using SCTST method from present *ab initio* calculations results and quantum thermal rate constants[30]. At high temperature, where anharmonic effects are less important, *e.g.*, in the range between 700 and 1100 K, the SCTST thermal rate constants from our *ab initio* calculations using harmonic effects are found to be in close agreement with the quantum calculations (Table-5), but our results deviate gradually from those with decreasing temperature.

TABLE-5
COMPARSION OF SCTST THERMAL RATE CONSTANTS (cm^3 $molecole^{-1}$ s^{-1}) FOR THE H + D_2 REACTION OF THIS WORK WITH QUANTUM RESULTS

T (K)	k (T) [Ref. 30][a]	k(T) QCISD[b]	k(T) QCISD[c]
300	4.9 (–19)	1.938 (–18)	2.212 (–18)
400	—	2.104 (–17)	2.346 (–17)
500	9.0 (–17)	1.027 (–16)	1.127 (–16)
600	—	3.152 (–16)	3.422 (–16)
700	8.1 (–16)	7.271 (–16)	7.828 (–16)
800	—	1.393 (–15)	1.494 (–15)
900	2.6 (–15)	2.350 (–15)	2.599 (–15)
1000	—	3.610 (–15)	3.853 (–15)
1100	5.4 (–15)	5.213 (–15)	5.530 (–15)

[a]Quantum results.
[b]Harmonic results of this work are in basis set cc-PVTZ.
[c]Basis set aug-cc-PVTZ.

The respective rate constants, k (T; v = 0, j = 0), CTST, TFTST with tunneling correction and with statistical factor and SCTST, are depicted as a function of the inverse of the temperature at the level QCISD with basis set cc-PVTZ and with basis set aug-cc-PVTZ, in Figs. 1 and 2, respectively and are compared to experimental values[30]. Figs. 1 and 2 show that CTST with tunneling can explain the experimental results at low temperature, as well as we can see that when statistical factor is applied to conventional transition state the correlation of experiment and

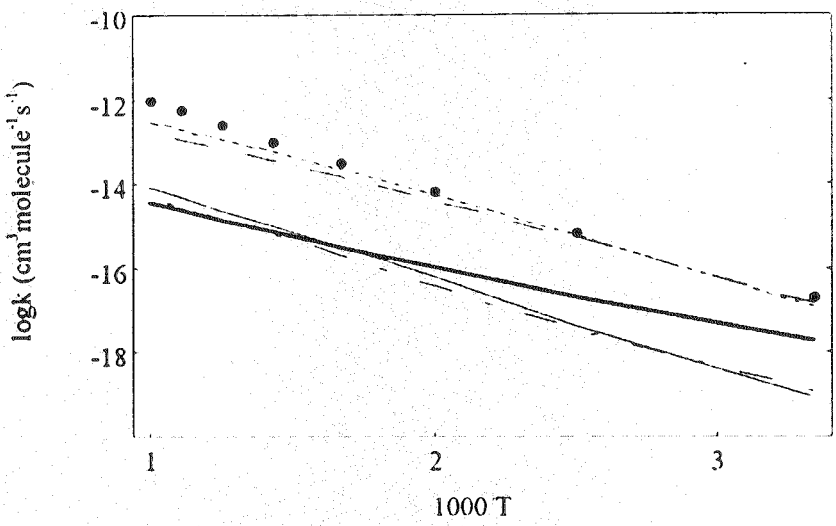

Fig. 1. Comparison of calculated and experimental rate constants for $H + D_2$ the collinear reaction. The points are the experimental results obtained from reference 30. The dashed and dotted lines are the results obtained from CTST with tunneling correction and statistical factor, respectively. The dot-dashed and solid lines are the results obtained from TFTST with tunneling correction and statistical factor, respectively. The solid line with thickness is the result obtained from SCTST calculations. These calculations are in the QCISD/cc-PVTZ

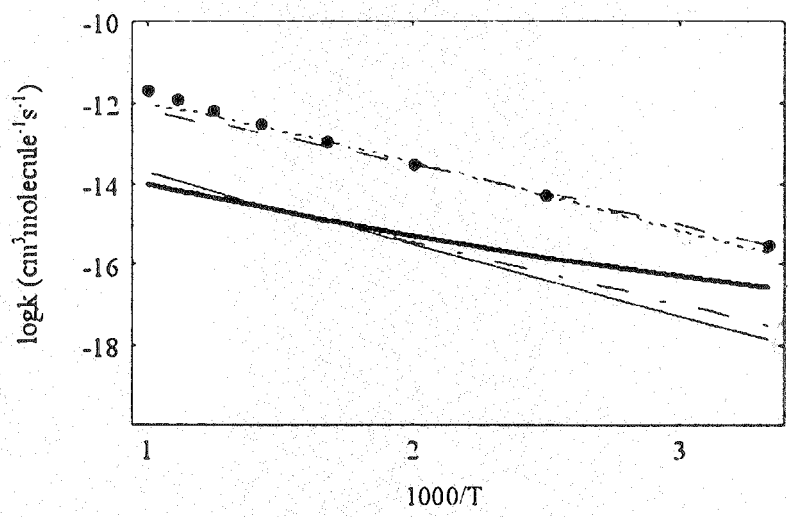

Fig. 2. Same as Fig. 1 except in the QCISD/aug-cc-PVTZ

theory is good, especially at high temperatures. This substantiates the fact that a tunneling correction should be applied in conventional transition state theory at low temperatures and a statistical factor at high temperatures where tunneling is not important. There are significant differences in the calculated rate constants using TFTST and SCTST methods with experimental and CTST results. The TFTST and SCTST k(T) calculated with our *ab initio* calculations are systematically lower than CTST ones and the experimental values. As shown in Figs. 1and 2, the rate constants obtained with QCISD level and basis sets cc-PVTZ and aug-cc-PVTZ are not quite similar to each other. The QCISD level with basis set aug-cc-PVTZ gives better results in rate constants compared to the QCISD level with basis set cc-PVTZ, so that the best accord between CTST rate constants and experiment is obtained at this level with basis set aug-cc-PVTZ.

Harmonic vibrational frequencies for reactant (H_2) and transition state (DH_2), electronic energies and thermal rate constants of D + H_2 reaction using three methods above are listed in Tables 6–10.

TABLE-6
AB INITIO MINIMUM-ENERGY GEOMETRIES AND VIBRATIONAL FREQUENCIES FOR THE D + H_2 REACTION

Properties			QCISD	
			cc-PVTZ[c]	aug-cc-PVTZ[d]
Bond length[a]	H_2		0.7426	0.7430
	TS		0.9301	0.9313
Frequencies[b]	H_2	ω	4409.3876	440.1477
	TS	ω_1	1773.8722	1765.3958
		ω_2	881.4997	848.0342
		ω_4	1459.0081	1459.1184

[a]Distances are in Å. Bond angle (H, X, H) is 90° and dihedral angle (H, X, H, D) is 180° for transition state (TS). The harmonic frequencies are in units of cm^{-1}.
[b]ω_1 = frequencies of symmetric stretch, ω_2 = frequencies of degenerate bend, ω_4 = frequencies of the imaginary reaction mode of transition state (DH_2).
[c]This work is in basis set cc-PVTZ.
[d]This work is in basis set aug-cc-PVTZ.

TABLE-7
AB INITIO ENERGIES FOR THE D + H_2 REACTION

Properties		QCISD	
		cc-PVTZ[c]	aug-cc-PVTZ[d]
Electronic energies	D + H_2	1.672146	1.672457
	TS	1.655777	1.656443
Reaction energies	E_0^a	10.271710	10.048750
	E_0^b	9.024848	8.705257

The electronic energies are in units hartrees (negative).
[a]The classical reaction energies (kcal mol^{-1}) do not include zero-point energies.
[b]The quantum reaction energies (kcal mol^{-1}) include zero-point energies.
[c]This work is in basis set cc-PVTZ.
[d]This work is in basis set aug-cc-PVTZ.

Calculated rate constants for this reaction using CTST, TFTS and SCTST methods are given as function of inverse of temperature at QCISD/cc-PVTZ and at QCISD/aug-cc-PVTZ in Figs. 3 and 4, respectively and are compared to experimental values[31]. The comparison of results for reaction $D + H_2$ is similar to that just discussed for the $H + D_2$.

Comparing $H + D_2$ with $D + H_2$ reaction, we can see that the rate constant of $H + D_2$ is smaller than $D + H_2$, especially in low temperature and it is attributed to the higher zero-point energy H_2 as compared with D_2.

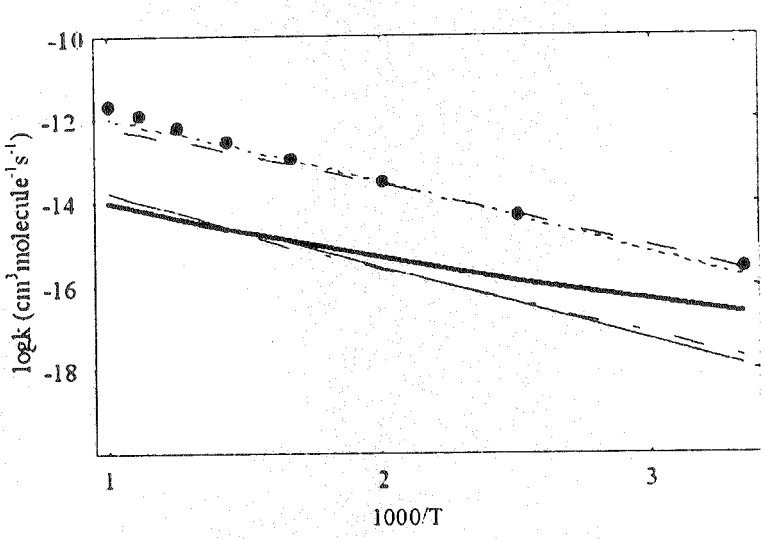

Fig. 3. Comparison of calculated and experimental rate constants for $D + H_2$ of the collinear reaction. The points are the experimental results obtained from reference 31. The dashed and dotted lines are the results obtained from CTST with tunneling correction and statistical factor, respectively. The dot-dashed and solid lines are the results obtained from TFTST with tunneling correction and statistical factor, respectively. The solid line with thickness is the result obtained from SCTST calculations. These calculations are in the QCISD/ cc-PVTZ

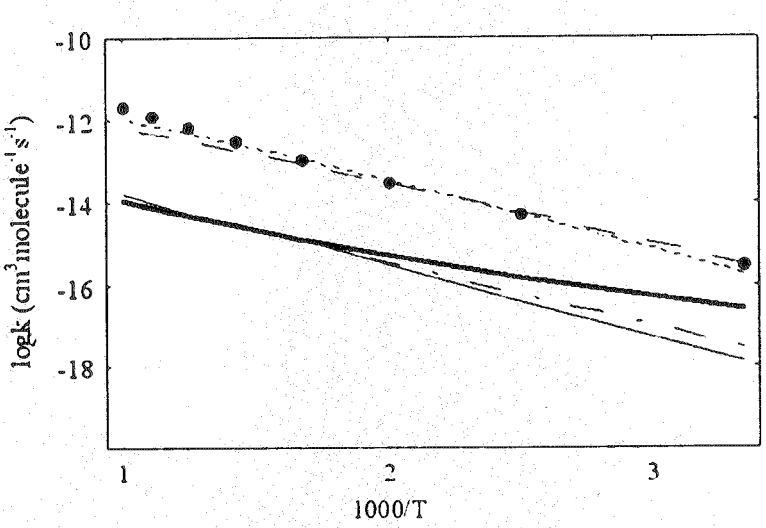

Fig. 4. Same as Fig. 3 except in the QCISD/aug-cc-PVTZ

TABLE-8
COMPARISON OF CTST RATE CONSTANTS (cm^3 $molecule^{-1}$ s^{-1}) FOR THE D + H_2 REACTION OF THIS WORK WITH OTHER RESULTS AND THE EXPERIMENT

T (K)	k(T) [Ref. 15]	k(T) [Ref. 22]	k(T) [Ref. 18]	k(T)[b] exp	k(T) QCISD[c]	k(T) QCISD[d]	k(T) QCISD[e]	k(T) QCISD[f]
300	3.3 (–16)[a]	1.87 (–16)	2.78 (–16)	2.96 (–16)	2.57 (–16)	1.62 (–16)	3.02 (–16)	1.89 (–16)
350	—	1.03 (–15)	—	1.47 (–15)	1.43 (–15)	1.09 (–15)	1.64 (–15)	1.25 (–15)
400	6.1 (–15)	3.79 (–15)	5.13 (–15)	5.11 (–15)	5.07 (–15)	4.51 (–15)	5.67 (–15)	5.04 (–15)
450	—	1.06 (–14)	—	1.39 (–14)	1.32 (–14)	1.33 (–14)	1.46 (–14)	1.46 (–14)
500	3.8 (–14)	2.47 (–14)	3.24 (–14)	3.17 (–14)	2.81 (–14)	3.09 (–14)	3.05 (–14)	3.36 (–14)
600	1.4 (–13)	9.04 (–14)	1.16 (–13)	1.15 (–13)	8.40 (–14)	1.06 (–13)	8.91 (–14)	1.13 (–13)
700	3.5 (–13)	2.36 (–13)	2.98 (–13)	3.07 (–13)	1.77 (–13)	2.47 (–13)	1.85 (–13)	2.57 (–13)
750	7.3 (–13)	3.51 (–13)	—	4.62 (–13)	2.36 (–13)	3.42 (–13)	2.45 (–13)	3.54 (–13)
800	—	4.98 (–13)	6.21 (–13)	6.67 (–13)	3.02 (–13)	4.51 (–13)	3.11 (–13)	4.65 (–13)
900	1.3 (–12)	9.06 (–13)	1.12 (–12)	1.26 (–12)	4.47 (–13)	7.03 (–13)	4.57 (–13)	7.17 (–13)
1000	2.1 (–12)	1.48 (–12)	1.83 (–12)	2.14 (–12)	6.03 (–13)	9.84 (–13)	6.11 (–13)	9.96 (–13)

[a]3.3 (–16) = 3.3×10^{-16}.
[b]The result obtained from Reference 31.
[c, d]This work is in basis set cc-PVTZ with tunneling correction and statistical factor, respectively.
[e, f]This work is in basis set aug-cc-PVTZ with tunneling correction and statistical factor, respectively.

TABLE-9
COMPARISON OF TFTST THERMAL RATE CONSTANT (cm^3 mol^{-1} s^{-1}) FOR THE D + H_2 REACTION OF THIS WORK WITH QUANTUM RESULTS

T (K)	k(T) [Ref. 18][a]	k(T) QCISD[b]	k(T) QCISD[c]	k(T) QCISD[d]	k(T) QCISD[e]
300	8.17 (–18)	1.997 (–18)	1.256 (–18)	3.157 (–18)	1.465 (–18)
400	—	4.254 (–17)	3.784 (–17)	2.703 (–17)	4.083 (–17)
500	5.22 (–16)	2.579 (–16)	2.839 (–16)	3.526 (–16)	3.084 (–16)
600	—	8.541 (–16)	1.082 (–15)	1.028 (15)	1.321 (–15)
700	3.00 (–15)	2.026 (–15)	2.825 (–15)	2.765 (–15)	2.891 (–15)
800	—	3.914 (–15)	5.844 (–15)	5.005 (–15)	5.035 (–15)
900	7.59 (–15)	6.464 (–15)	1.015 (–14)	7.079 (–15)	1.023 (–14)
1000	—	1.013 (–14)	1.652 (14)	1.023 (–14)	1.656 (–14)

[a]Quantum results.
[b, c]This work is in basis set cc-PVTZ with tunneling correction and statistical factor, respectively.
[d, e]This work is in basis set aug-cc-PVTZ with tunneling correction and statistical factor, respectively.

TABLE-10
COMPARISON OF SCTST THERMAL RATE CONSTANTS (cm^3 $molecule^{-1}$ s^{-1}) FOR THE D + H_2 REACTION OF THIS WORK WITH OTHER RESULTS

T (K)	k(T) [Ref. 18][a]	k(T) [Ref. 17][b]	k(T) QCISD[c]	k(T) QCISD[d]
300	8.17 (–18)	9.2 (–18)	2.29 (–17)	2.67 (–17)
400	—	—	1.31 (–16)	1.49 (–16)
500	5.22 (–16)	5.6 (–16)	4.57 (–16)	5.13 (–16)
600	—	—	1.16 (–15)	1.28 (–15)
700	3.00 (–15)	3.2 (–15)	2.36 (–15)	2.58 (–15)
800	—	—	4.15 (–15)	4.51 (–15)
900	7.59 (–15)	8.1 (–15)	6.57 (–15)	7.10 (–15)
1000	—	—	9.63 (–15)	1.04 (–14)
1100	1.33 (–14)	1.4 (–14)	1.33 (–14)	1.43 (–14)

[a, b]Quantum results.
[c]Harmonic results of this work are in basis set cc-PVTZ.
[d]Basis set aug-cc-PVTZ.

REFERENCES

1. B.A. Ridley, W.R. Schulz and D.J. Le Roy, *J. Chem. Phys.*, **44**, 3344 (1966); D.J. Le Roy, B.A. Ridley and K.A. Quickert, *Disc. Faraday Soc.*, **44**, 92 (1967); D.N. Mitchell and D.J. Le Roy, *ibid.*, **58**, 3449 (1973).
2. A.A. Westenberg and N. De Haas, *J. Chem. Phys.*, **47**, 1393 (1967).
3. K.A. Quickert and D.J. Le Roy, *J. Chem. Phys.*, **54**, 5444 (1971).
4. I. Jayaweera and P.D. Pacey, *J. Phys. Chem.*, **94**, 3614 (1990).
5. J.V. Michael, *J. Chem. Phys.*, **92**, 3394 (1990).
6. J.V. Michael and J.R. Fisher, *J. Phys. Chem.*, **94**, 3318 (1990); J.V. Michael, J.R. Fisher, J.M. Bowman and Q. Sun, *Science*, **249**, 269 (1990).
7. V.B. Rozenshtein, Y.M. Gershenzon, A.V. Ivanov, S.D. Il'in and S.I. Kucheryavii, *Chem. Phys. Lett.*, **105**, 423 (1984) and references therein.
8. H. Buchenau, J.P. Toennies, J. Arnold and J. Wolfrum, *J. Ber. Bunsen-Ges. Phys. Chem.*, **94**, 1231 (1990) and references therein.
9. R.N. Porter and M. Karplus, *J. Chem. Phys.*, **40**, 1105 (1964).
10. R.N. Porter and M. Karplus, *Disc. Faraday Soc.*, **44**, 164 (1967).
11. D.G. Truhlar and C.J. Horowitz, *J. Chem. Phys.*, **68**, 2466 (1978); **71**, 1514 (1979).
12. H.R. Mayne and J.P. Toennies, *J. Chem. Phys.*, **75**, 1794 (1981).
13. B.C. Garrett and D.G. Truhlar, *J. Chem. Phys.*, **72**, 3460 (1980).
14. S. Takada, A. Ohsaki and H. Nakamura, *J. Chem. Phys.*, **96**, 339 (1992).
15. D. Wang and J.M. Bowman, *J. Phys. Chem.*, **98**, 7994 (1994).
16. B.C. Garrett, D.G. Truhlar, A.J.C. Varandas and N.C. Blais, *Int. J. Chem. Kinet.*, **18**, 1065 (1986) and references therein.
17. T.J. Park and J.C. Light, *J. Chem. Phys.*, **94**, 2946 (1991).
18. S.L. Mielke, G.C. Lynch, D.G. Truhlar and D.W. Schwenke, *J. Phys. Chem.*, **98**, 8000 (1994).

19. A.J.C. Varandas, F.B. Brown, C.A. Mead, D.G. Truhlar and N.C. Blais, *J. Chem. Phys.*, **86**, 6258 (1987).
20. A.I. Boothroyd, W.J. Keogh, P.G. Martia and M.R. Peterson, *J. Chem. Phys.*, **95**, 4343 (1991).
21. S.M. Auerbach and W.H. Miller, *J. Chem. Phys.*, **100**, 1103 (1994).
22. F.J. Aoiz, L. Banares, T. Diez-Rojo, V.J. Herrero and V.S. Rabanos, *J. Phys. Chem.*, **100**, 4071 (1996).
23. T. Yamamoto and W.H. Miller, *J. Chem. Phys.*, **118**, 2135 (2003).
24. M.J. Cohen, N.C. Handy, R. Hernandez and W.H. Miller, *Chem. Phys. Lett.*, **192**, 407 (1992).
25. M. Dehestani and F. Shojaie, *Asian J. Chem.*, **17**, 1863 (2005).
26. M.J. Frisch, G.W. Trucks, H.B. Schlegel, G.E. Scuseria, M.A. Robb, J.R. Cheeseman, V.G. Zakrzewsi, J.A. Montgomery, R.E. Stratmann, J.C. Burant, S. Dapprich, J.M. Millam, A.D. Daniels, K.N. Kudin, M.C. Strain, O. Farkas, J.Tomasi, V. Barone, M. Cossi, R. Cammi, B. Mennucci, C. omelli, C. Adamo, S. Clifford, J. Ochterski, G.A. Petersson, P.Y. Ayala, Q. Cui, K Morokuma, D.K. Malick, A.D. Rabusk, K. Raghavachari, J.B. Foresman, J. Ciosłowski, J.V. Ortiz, B.B. Stefanov, G. Liu, A. Liashenko, P. Piskorz, I. Komaromi, R. Gomperts, R.L. Martin, D.J. Fox, T. Keith, M.A. L. Laham, C.Y. Peng, A. Nanayakkara, C. Gonzalez, M. Challacombe, P.M.W. Gill, B.G. Johnson, W. Chen, M.W. Wong, J.L. Andres, M. Head-Gordon, E.S. Replogle and J.A. Pople, GAUSSIAN 98, Revision A. 3, Gaussian Inc., Pittsburgh, PA (1998).
27. T.J. Park and J.C. Light, *J. Chem. Phys.*, **96**, 8850 (1992).
28. B.C. Garrett and D.G. Truhlar, *J. Chem. Phys.*, **72**, 3460 (1980).
29. J.V. Michael and J.R. Fisher, *J. Phys. Chem.*, **92**, 3394 (1990).
30. K.A. Quickert and D.J. Le Roy, *J. Chem. Phys.*, **53**, 1325 (1970).
31. J.V. Michael, *J. Phys. Chem.*, **94**, 3318 (1990).

(*Received*: 7 November 2005; *Accepted*: 3 March 2006) AJC-4712